

Upper critical field and fluctuation conductivity in the critical regime of doped SmFeAsO

I.Pallecchi ^a, C.Fanciulli ^a, M.Tropeano ^a, A.Palenzona ^b, M.Ferretti ^b, A.Malagoli ^a, A.Martinelli ^b, I.Sheikin ^c, M.Putti ^{a,d}, C.Ferdeghini ^a

^a *CNR-INFM-LAMIA and Università di Genova, via Dodecaneso 33, 16146 Genova, Italy*

^b *DCCI, Università di Genova and CNR-IMEM unità di Genova, via Dodecaneso 31, 16146 Genova, Italy*

^c *GHMFL, MPI-FKF/CNRS, 28 Avenue des Martyrs, BP 166, 38042 Grenoble, France*

^d *ASC, NHMFL, FSU, 2031 E. Paul Dirac Dr., Tallahassee, FL 3231, USA*

Abstract

We measure magnetotransport of F doped SmFeAsO samples up to 28T and we extract the upper critical fields, using different criteria. In order to circumvent the problem of criterion-dependence H_{c2} values, we suggest a thermodynamic estimation of the upper critical field slope dH_{c2}/dT based on the analysis of conductivity fluctuations in the critical regime. A high field slope as large as $-12T/K$ is thus extracted for the optimally doped sample. We find evidence of a two-dimensional lowest Landau level (LLL) scaling for applied fields larger than $\mu_0 H_{LLL} \sim 8T$. Finally, we estimate the coherence length values and we observe that they progressively increase with decreasing T_c . In all cases, the coherence length values along the c axis are smaller than the interplanar distance, confirming the two-dimensional nature of superconductivity in this compound.

Introduction

Since the recent discovery of superconductivity with $T_c=26\text{K}$ in doped LaFeAsO ¹, the class of these iron-based oxypnictides has been object of intensive research, which have lead to the current record of $T_c=56\text{K}$ ². In compounds with general chemical formula REFeAsO ($\text{RE}=\text{La}, \text{Sm}, \text{Nd}, \text{Ce}\dots$), it is believed that doped REO layers act as charge reservoirs for high mobility FeAs planes, making oxypnictides very similar to the layered structure of high- T_c cuprates. Beyond the theoretical challenge of understanding the unconventional pairing mechanism responsible for superconductivity, many studies have been devoted to superconductive properties of applicative appeal, such as the huge values of the upper critical field and its dependence on the particular rare earth RE³. Slopes of $H_{c2}(T)$ as large as about -9.3T/K have been measured in compounds with Sm. Such high $H_{c2}(T)$ implies a short coherence length that, together with the high T_c , the layered structure and the rather anisotropic Fermi surface, make these compounds candidate to present enhanced thermal fluctuations. In the case of the $\text{RE}=\text{Nd}$ compound, coherence lengths along the c axis, ξ_c varying from 0.26 to 0.9 nm have been evaluated^{4,5,6} which are lower or comparable to the distance between the FeAs-layers. The occurrence of remarkable thermal fluctuations, indeed, has been observed by specific heat analysis.

The investigation of thermal fluctuation effects may offer several hints for the comprehension of these compounds. The identification of three-dimensional (3D) rather than two-dimensional (2D) thermal fluctuations is a crucial point, because the latter could imply the occurrence of pronounced dissipation in the mixed state, detrimental for applications, as observed in cuprates.

Among the oxypnictides, $\text{SmFeAs}(\text{O}_{1-x}\text{F}_x)$ presents high T_c ($\sim 54\text{K}$ ^{3,7,8}), the largest slope of $H_{c2}(T)$ and high anisotropy^{9,10} which make this compound the most suitable for investigating fluctuation effects. In turns, however, due to the expected fluctuation contribution just above T_c , there is not univocal consensus about the criterion for the extraction of the upper critical field from transport experimental data. Alternatively, a thermodynamic determination of the transition temperature at different magnetic fields has been proposed which is thought to reflect an intrinsic behavior of the material; in this analysis, lower H_{c2} slopes and consequently larger coherence lengths have been evaluated.

The same problem has been met with cuprates and the analyses of fluctuation effects of conductivity, specific heat, magnetization, Ettinghausen, Hall and Nernst effects have been suggested to provide a reliable tool for this aim, provided that fluctuation effects are significant in an appreciable temperature range around $T_c(H)$. Fluctuation effects are quantified by the Ginzburg number, which can be expressed for a 3D superconductor by $Gi_{3D}=(\pi\kappa^2\xi_0K_B T_c\mu_0/2\Phi_0^2)^2$ and, in presence of a magnetic field, by its magnetic field dependent counterpart¹¹ $Gi_{3D}(H)=(2H\cdot Gi_{3D}^2/H_{c2})^{2/3}$, where $\kappa=\lambda_0/\xi_0$ is the Ginzburg-Landau parameter, λ_0 is the London penetration depth, ξ_0 is the coherence length, H_{c2} is the zero temperature limit of the upper critical field, K_B is the Boltzmann constant, H the applied magnetic field and Φ_0 is the flux quantum. In conventional superconductors $Gi_{3D}\sim 10^{-5}$, while in high- T_c cuprates it is $\sim 10^{-3}-10^{-2}$, making fluctuations significant in an experimentally accessible temperature window $\sim Gi_{3D}\cdot T_c$; experimental results indicate that the actual temperature window of fluctuations is even larger than this estimate. In the $\text{RE}=\text{Sm}$ compound, assuming $T_c\approx 54\text{K}$, $\lambda\approx 190\text{nm}$ ^{12,13} and $\xi_c\approx 0.6\text{nm}$, which is an average value for the $\text{RE}=\text{Nd}$ compound, we estimate $Gi_{3D}\sim 8\cdot 10^{-3}$, so that a similar situation to the case of high- T_c cuprates occurs. For a 2D superconductor, that could be more appropriate for the case of $\text{SmFeAs}(\text{O}_{1-x}\text{F}_x)$, the Ginzburg number can be expressed as $Gi_{2D}=K_B T_c/E_F$ ¹⁴. From Hall effect and effective mass data of ref. , this yields approximately $Gi_{2D}\approx 0.01$, a remarkably high value.

In this paper, we measure magnetotransport $\text{SmFeAs}(\text{O}_{1-x}\text{F}_x)$ samples with different doping x , in magnetic fields up to 28 T. From the analysis of conductivity fluctuations in high fields, in the critical regime close to and below the transition temperature, we find evidence of 2D behavior and we extract the high field linear slope of the upper critical field $H_{c2}(T)$, which is as large as

$dH_{c2}/dT \approx -12T/K$ in the most doped sample and progressively decreases with decreasing T_c . Consequently the coherence lengths values increase, still remaining smaller than the interplanar distance, which confirms the 2D nature of superconductivity in these compounds.

Fluctuation conductivity in the critical regime

The classical theory of fluctuations near T_c (hereafter, throughout the treatment of fluctuation effects, the transition temperature T_c must be intended as the mean field transition temperature) predicts that the fluctuation conductivity $\Delta\sigma$ due to finite Cooper pair formation above T_c is described in the 3D and 2D cases by^{15,16} $\Delta\sigma_{3D} \propto \varepsilon^{-1/2}$ and $\Delta\sigma_{2D} \propto \varepsilon^{-1}$ laws, respectively, where $\varepsilon = \ln(T/T_c) \approx (T - T_c)/T_c$. In the Lawrence-Doniach picture for layered systems¹⁷, a crossover from 2D to 3D behavior is expected to occur approaching T_c , due to the divergence of the coherence length. Within this Gaussian approximation, the fluctuation conductivity is therefore predicted to diverge close to the transition temperature. This nonanalyticity is removed if interactions between fluctuations are taken into consideration, which is necessary in the so called critical regime, that is in a region of the T_c -H phase diagram close to $T_c(H)$. The temperature range in which critical fluctuations should be observed is proportional to ξ_0^{-6} in the 3D case, that is an experimentally accessible range of the order of 1K for high- T_c superconductors¹⁸. In a magnetic field this range is expected to increase further as $\sim H^{2/3}$ or $\sim H^{1/2}$ in 3D and 2D, respectively¹⁹.

In the critical regime, in the limit of strong magnetic fields, a scaling form for thermodynamic functions is expected. If quasiparticles are confined in the lowest Landau level (LLL), transport becomes of one-dimensional (1D) character along the direction of the applied field. Fluctuation effects close to the superconducting transition are further enhanced by the lower effective dimensionality of the system. Ullah and Dorsey^{20,21} calculated the fluctuation conductivity $\Delta\sigma$ including the free energy quartic term within the Hartree approximation and obtained a scaling law for $\Delta\sigma$ in magnetic fields, in terms of unspecified scaling functions F_{2D} and F_{3D} , valid for 2D and 3D superconductors, respectively:

$$\Delta\sigma(H)_{2D} = \left(\frac{T}{H}\right)^{1/2} F_{2D} \left(A \frac{T - T_c(H)}{\sqrt{T \cdot H}} \right) \quad (1.a)$$

$$\Delta\sigma(H)_{3D} = \left(\frac{T^2}{H}\right)^{1/3} F_{3D} \left(B \frac{T - T_c(H)}{(T \cdot H)^{2/3}} \right) \quad (1.b)$$

where A and B are characteristic constants of the material. Such functional dependence still holds even if more than one (but only a few) higher Landau levels are involved, as long as the inter-LL interaction is negligible^{22,23}. However the scaling cannot account for the shape of the resistive transition in case the broadening is due to the dissipative flux line motion rather than to fluctuation effects. The field H_{LLL} above which the LLL approximation should hold fulfils the condition that the Landau level spacing is larger than the Landau level interaction energy. According to Tešanović and coworkers²², this condition is translated as $H_{LLL} \sim (Gi/16)(T/T_{c0})H_{c2}(0)$, with $T_{c0} = T_c(H=0)$. More practically, they suggest the thumb rule $H_{LLL} \sim H_{c2}/3$.

The LLL scaling has been successfully applied to high- T_c cuprates. Polycrystalline samples^{27,24} display similar behavior as single crystals. A 3D behavior has been observed in the case of $YBa_2Cu_3O_x$ ^{25,26,24} and a 2D one in the case of $Tl_2Ba_2CaCu_2O_x$ ²⁷ and $Bi_2Sr_2CaCu_2O_8$ ²⁸. $\mu_0 H_{LLL}$ values are found to range from 1T^{25,27,29,24} to $\sim 10T$ ^{30,26} for high- T_c cuprates.

Experimental magnetotransport results

We prepare polycrystalline $SmFeAs(O_{1-x}F_x)$ samples with nominal doping $x=0.07$, 0.1 and 0.15 following the steps described in³¹: once SmAs is synthesized from pure elements, it is reacted

with stoichiometric amounts of Fe, Fe₂O₃, and FeF₂ at high temperature. Single phase formation is checked in all the samples by X-rays analysis.

Resistivity measurements from 4K to 300K are carried out in magnetic fields up to 9 T in a PPMS Quantum Design system and up to 28 T at Grenoble High Magnetic Field Laboratory.

In the left-hand panel of figure 1, we present resistivity curves normalized at $\rho(300\text{K})$ of the three SmFeAs(O_{1-x}F_x) samples analyzed in this paper. It can be seen that the resistivity curves exhibit metallic behavior, with a tendency to saturate above $\sim 160\text{K}$. Below this temperature ρ decreases linearly with temperature and its slope progressively decreases with decreasing T_c of the sample, with a monotonic tendency to a weaker metallicity from the optimally doped to the underdoped sample.

The superconducting transitions are quite rounded, making it difficult to univocally determine the transition temperatures and width. In Table I the values of T_c obtained by the criterion of 50% resistivity drop and of ΔT_c obtained as the temperature interval between 90% and 10% resistivity drops are listed. The $x=0.15$ sample presents $T_c=51.5\text{ K}$, the $x=0.1$ sample $T_c=41.5\text{ K}$ and the least doped sample $T_c=33\text{ K}$.

In the three right-hand panels of figure 1, the zoomed transition regions in magnetic fields from zero to 28T for the three samples are shown. The typical fan-shaped broadenings of the transitions are well visible for all the samples, indicating an important contribution of fluctuations.

From these magnetotransport data, we extract the characteristic critical fields, using different criteria. The criterion proposed in ref. ³² consists in finding the intersection $\rho^*(T^*)$ between linear extrapolations of the $\rho(T)$ curves above and below T_c . Hence, the temperatures at which the resistivity is 90% and 10% of ρ^* allow to trace $H_{90\%}^*(T)$ and $H_{10\%}^*(T)$, respectively. Another common criterion consists on extrapolating linearly the normal state resistivity, then trace the parallel straight lines at 90% and 10% of the normal state extrapolation and find the respective intercepts with the $\rho(T)$ curves; this procedure identifies $H_{90\%}(T)$ and $H_{10\%}(T)$, respectively. In figure 2, we plot all the above critical fields for the three samples. In Table II we report the values of the high field ($\geq 8\text{T}$) linear slopes of such critical fields. Those extracted from the tails are believed to represent the irreversibility fields, and have similar values for all the samples, around $-2\text{T/K} \div -3\text{T/K}$, depending on the used criterion. The critical fields extracted from the onsets of the transitions represent the upper critical fields H_{c2} . As transport always follows the less resistive path, in polycrystalline samples with randomly oriented grains, the measured upper critical fields are the largest ones, that is those of the grains whose c axis is perpendicular to the applied field (usually labeled $H_{c2\parallel ab}$). These upper critical field slopes vary from $-5\text{T/K} \div -20\text{T/K}$, depending on the criterion. However, by inspecting Table II it is clear that the variations due to different criteria are comparable to the variations from sample to sample. This sensitivity to the used criterion makes it also difficult to compare different values in literature. In the next section, we propose a criterion to extract a thermodynamic H_{c2} , that is based in conductivity fluctuations in the critical regime.

Experimental fluctuation conductivity results

We extract the fluctuation conductivity $\Delta\sigma$ as the difference between the normal state conductivity σ_n and the measured conductivity σ . The former σ_n is obtained from extrapolation of the resistivity measured in a temperature interval suitably chosen for each sample, roughly 30K around $2T_c$, where fluctuation contribution is assumed to be negligible. For the three samples, $\Delta\sigma$ in zero field as a function of ε are plotted in the insets of figure 3; therein, the solid lines indicate the 2D asymptotic behavior $\Delta\sigma_{2D} \propto \varepsilon^{-1}$. In the Gaussian regime, not too close to the transition ($0.01 < \varepsilon < 0.1$), $\Delta\sigma$ exhibits a well defined asymptotic 2D behavior $\propto \varepsilon^{-1}$, delimited at either sides by sharp crossovers to the critical regime for $\varepsilon < 0.01$ and the high-temperature short-wavelength regime

for $\varepsilon > 0.1$.³³ It can be also seen that the 2D behavior $\Delta\sigma_{2D} \propto \varepsilon^{-1}$ is extended up to $\varepsilon \sim 0.1$, which means 3 to 5K above T_c (it is worth noting that T_c values extracted by this fluctuation analysis fall very close to the 50% resistivity drop values reported in Table I). This interval is larger than the transition widths and the presence of some inhomogeneity, which may yield a distribution of T_c , does not mask the characteristic behavior of Gaussian fluctuations. However, to avoid possible ambiguities yielded by any T_c distribution, in the following of the paper we focus on the shape of the critical fluctuation conductivity at high fields; in this regime, the LLL scaling is not affected by a relatively small T_c distribution, but rather accounts for the in-field broadening of the transition, which is huge in our samples. For example, in the sample S3, $\Delta T_c(H=0) \sim 2K$ becomes as large as 7K at 8T and 17K at 28T.

In order to verify the 2D nature of fluctuations, in the main panels of figure 3, we plot $\Delta\sigma \cdot (H/T)^{1/2}$ versus $(T-T_c(H))/(T \cdot H)^{1/2}$, expected for the 2D LLL scaling, for the three samples. It is apparent that the 2D scaling succeeds in making the curves collapse in an extended temperature range and for fields above $\mu_0 H_{LLL} \sim 8T$. To compare the 2D with the 3D scaling in figure 4, according to equations (1.a) and (1.b), we plot the $\Delta\sigma \cdot (H/T)^{1/2}$ versus $(T-T_c(H))/(T \cdot H)^{1/2}$, expected for the 2D LLL case (left-hand panel) and $\Delta\sigma \cdot H^{1/3}/T^{2/3}$ versus $(T-T_c(H))/(T \cdot H)^{2/3}$ expected for the 3D LLL case (right-hand panel) for the one of the samples as representative of all, S2, in linear (main panels) and semilogarithmic (insets) scales. The maximum and minimum values of the horizontal axes for the 2D and 3D cases are chosen so that they correspond to the same temperature interval. The 2D relationship provides a better scaling of data both below and above T_c ; indeed, in the 3D case, the curves at different fields open like a fan above T_c and tend to depart from each other also below T_c . On the contrary, in the 2D case, the curves above 6T overlap almost in the whole range, being the broadening simply due to random scattering of experimental data. 2D character means that the relevant coherence length ξ_c is smaller than the inter-plane spacing, or, equivalently, that the Josephson coupling between adjacent superconducting planes is smaller than intraplane condensation energy. The success of the scaling also indicates that the fan-shaped transitions displayed in figure 1 are primarily due to thermodynamic fluctuations of the superconducting order parameter, rather than to dissipative motion of flux lines. The latter effect may indeed come into play at low negative values of the variable in the horizontal axes $(T-T_c(H))/(T \cdot H)^{1/2}$, where the fluctuation conductivity curves start to depart from one another. This occurs several degrees K below T_c , just at the tail of the transitions.

The crossover value $\mu_0 H_{LLL} \sim 8T$ is worth some considerations. In $YBa_2Cu_3O_x$, lower values are generally found.^{25,24,34} The criterion proposed by Tešanovič²² $H_{LLL} \sim H_{c2}/3$ suggests that the higher upper critical fields of $SmFeAsO_{1-x}F_{1-x}$ as compared to those of $YBa_2Cu_3O_x$ may account for the difference in the H_{LLL} values.

We can use the validity of the 2D LLL scaling to extract $T_c(H)$, treated as fitting parameter. The so obtained thermodynamic H_{c2} curves are reported in Table II and shown as a function of temperature in figure 2, together with the H_{c2} curves extracted from other criteria. Remarkable values of the thermodynamic $\mu_0 H_{c2}$ linear slope at high fields are found, namely -12T/K for S3, -7.5T/K for S2 and -7T/K for S1. The value of -12 T/K obtained in the most doped sample is the largest reported for oxypnictides. With such dH_{c2}/dT value, the single band Werthamer-Helfand-Hohenberg (WHH) formula³⁵ yields in the zero temperature limit $\mu_0 H_{c2} \approx 0.693 T_c |\mu_0| dH_{c2}/dT|_{T_c} \approx 400T$. This huge upper critical field is well above the paramagnetic limit and suggests that a Pauli limiting behavior should be evident in these compounds at high fields³⁶.

With decreasing T_c the slope values progressively decrease; this is in disagreement with what was observed in $LaFeAsO$ where H_{c2} evaluated with the 80% criterion has been found to follow a non monotonic trend with T_c .³⁷ In conventional superconductors such as A-15 and MgB_2 ,³⁸ dH_{c2}/dT increases with decreasing T_c because the T_c reduction is often accompanied by an increase of disorder that carries the superconductor into the dirty limit. In short coherence length superconductors like high- T_c cuprates, the dirty limit is not likely achieved and effects related to the doping prevail. This might be the case of oxypnictides, even if disorder effects on H_{c2} have been

suggested for $\text{LaFeAsO}_{0.9}\text{F}_{0.1}$. However, lower H_{c2} values of RE=La as respect to the RE=Sm compounds indicate that the latter should present lower intrinsic coherence length, more unlikely affected by disorder. If we neglect disorder effects, the simultaneous reduction of dH_{c2}/dT and T_c can be explained by a reduction of the coupling that suppresses both the properties.

From H_{c2} slope values, taking into account that in polycrystals H_{c2} parallel to the ab-planes is actually probed and assuming an anisotropy factor $\gamma=\xi_{ab}/\xi_c$ ranging from 5 to 9^{9,10} the coherence lengths can be evaluated by means of the upper critical field obtained from the WHH formula. In Table III, the values for all the samples are calculated. Despite the large uncertainty on the anisotropy factor γ which includes also a possible dependence of γ on doping, we notice that the average values of ξ_{ab} increase remarkably from ~ 23 Å to ~ 37 Å and those of ξ_c increase from ~ 3.4 Å to 5.5 Å from sample S3 to S1. This suggests that moving from optimal to underdoped regimes a crossover from 2D to 3D regime could occur, even if in our case ξ_c remains always smaller than the interplanar spacing $s=8$ Å, confirming the 2D nature of superconductivity in the measured samples.

An opposite behavior was observed in $\text{YBa}_2\text{Cu}_3\text{O}_x$ where thermal fluctuations change from 2D to 3D nature moving from the underdoped to the optimally doped regime.^{39,40} This opposite trend implies an important difference between oxypnictides and high- T_c cuprates. In the latter ones, the doping changes substantially the transport properties from insulating to metallic and increases the coupling between the conducting planes. As a consequence, with increasing doping, the anisotropy progressively decreases and when its value is such that $\xi_c=\xi_{ab}/\gamma$ becomes comparable to the interlayer spacing a crossover from 2D to 3D fluctuation regime occurs. Oxypnictides are metallic compounds: fluorine doping determines the occurrence of superconductivity by breaking symmetries of the Fermi surface, but it does not change substantially the transport properties⁴¹ and anisotropy it is not expected to change substantially. Thus, a possible crossover from 2D to 3D fluctuation regime with doping could only be driven by the progressive increase of the coherence length with decreasing T_c .

Conclusions

We study fluctuation conductivity in F doped SmFeAsO polycrystalline samples, in the critical regime close and below $T_c(H)$. At fields above $\mu_0 H_{LLL} \sim 8T$, the conductivity curves obey the 2D LLL scaling, similarly to the BSSCO superconductor family. Such scaling allows to extract a thermodynamic estimation of the upper critical field, whose high field slope is as large as $-12T/K$ in the most doped sample, in fair agreement with the values extracted with the criterion of 90% drop of the resistivity from its normal state value. The corresponding coherence lengths along the c axis turn out to be from 3 Å to 6 Å, always smaller than the interplanar spacing $s=8$ Å, consistently with the 2D nature of superconductivity in these compounds.

Acknowledgements

This work is partially supported by Compagnia di S. Paolo and by the European Commission from the 6th framework programme "Transnational Access - Specific Support Action", contract N° RITA-CT-2003-505474 and by the Italian Foreign Affairs Ministry (MAE) - General Direction for the Cultural Promotion. The authors are grateful to A.Gurevich for helpful discussion.

Figure and table captions

Table I: Properties of the SmFeAs(O_{1-x}F_x) samples: nominal doping x; transition temperature T_c, defined as the temperature at which the resistivity drops to 50% of its extrapolated normal state value and transition width ΔT_c, defined as the temperature interval between 90% and 10% resistivity drops with respect to its extrapolated normal state value.

Table II: Linear slopes of the critical fields above 8T, extracted using different criteria, as explained in the text. In the last column are the slopes extracted from the LLL fitting of the fluctuation conductivity.

Table III: Values of the coherence length parallel and perpendicular to the superconducting planes ξ_{ab} and ξ_c in Å calculated from the WHH formula; the variability ranges are related to the range of literature values found for the anisotropy γ=ξ_{ab}/ξ_c≈5÷9.

Figure 1: (color online) Resistivity versus temperature curves of the three SmFeAs(O_{1-x}F_x) samples in zero magnetic field (left-hand panel) and in magnetic fields up to 28T (right-hand panels). Due to an unknown geometric factor related to the sample density, resistivity absolute values suffer of an uncontrolled uncertainty and they have been normalized to their T=300K values.

Figure 2: (color online) Critical fields extracted from the in-field resistivity curves of the three samples, using different criteria (see text).

Figure 3: (color online) In the main panels, the plots of the quantity Δσ·(H/T)^{1/2} versus (T-T_c(H))/(T·H)^{1/2} for the three samples demonstrate the success of the 2D LLL scaling; in the insets, the curves of fluctuation conductivity Δσ versus ε=ln(T/T_c) in the Gaussian regime and zero magnetic field are shown, together with the asymptotic 2D behavior Δσ_{2D}∝ε⁻¹ indicated by continuous lines.

Figure 4: (color online) In the main panels, the plots of the quantity Δσ·(H/T)^{1/2} versus (T-T_c(H))/(T·H)^{1/2} (left-hand) and Δσ·(H/T²)^{1/3} versus (T-T_c(H))/(T·H)^{2/3} (right-hand) expected for the 2D LLL and 3D LLL cases, respectively, are shown for the sample S2. In the insets, the same plots are displayed in semilogarithmic scale.

Table I:

Sample	x	$T_c \pm \Delta T_c/2$ (K)
S1	0.07	33.0 ± 1.5
S2	0.10	41.5 ± 1
S3	0.15	51.5 ± 1

Table II:

Sample	$\mu_0 dH^*_{10\%}/dT$ (T/K)	$\mu_0 dH_{10\%}/dT$ (T/K)	$\mu_0 dH^*_{90\%}/dT$ (T/K)	$\mu_0 dH_{90\%}/dT$ (T/K)	$\mu_0 dH_{flut}/dT$ (T/K)
S1	-2.8	-2.4	-5.8	-5.3	-7.0 ± 1
S2	-3.7	-2.3	-7.3	-7.1	-7.5 ± 1
S3	-3.6	-1.7	-20.7	-11.3	-12 ± 1

Table III:

Sample	ξ_{ab} (Å)	ξ_c (Å)
S1	31÷42	6.3÷4.7
S2	27÷37	5.4÷4.1
S3	19÷26	3.9÷2.9

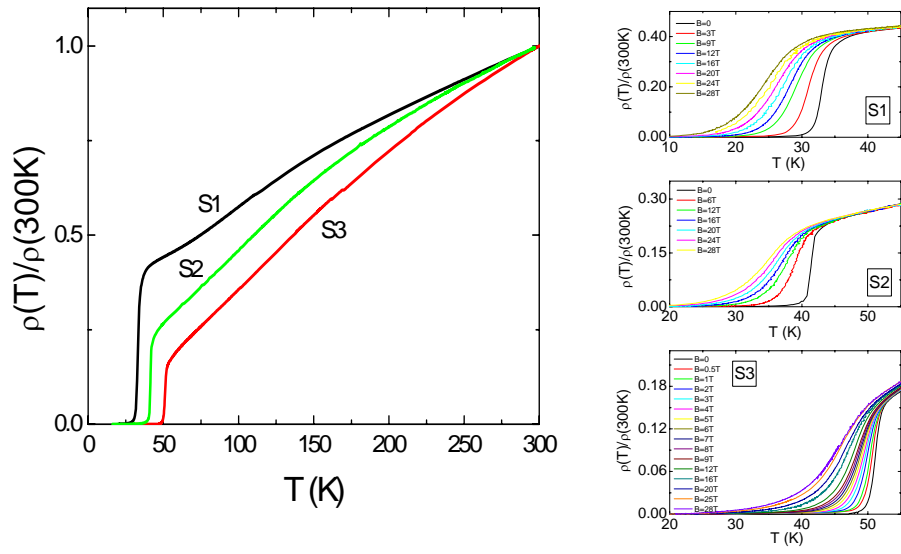


Figure 1

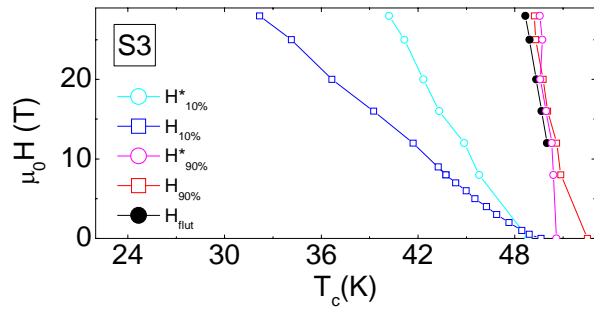
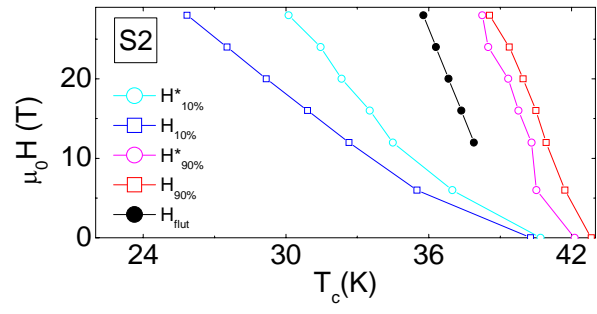
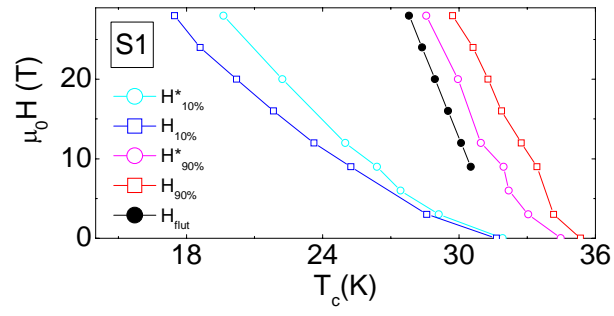


Figure 2

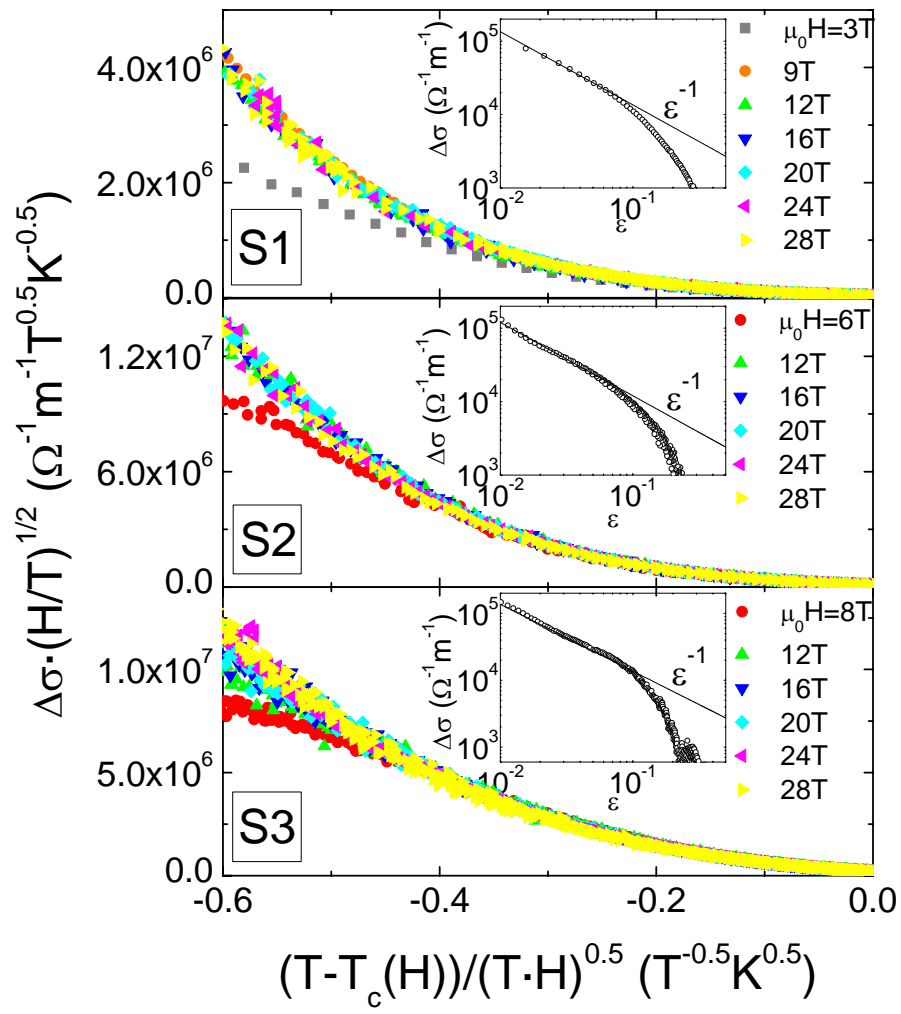


Figure 3

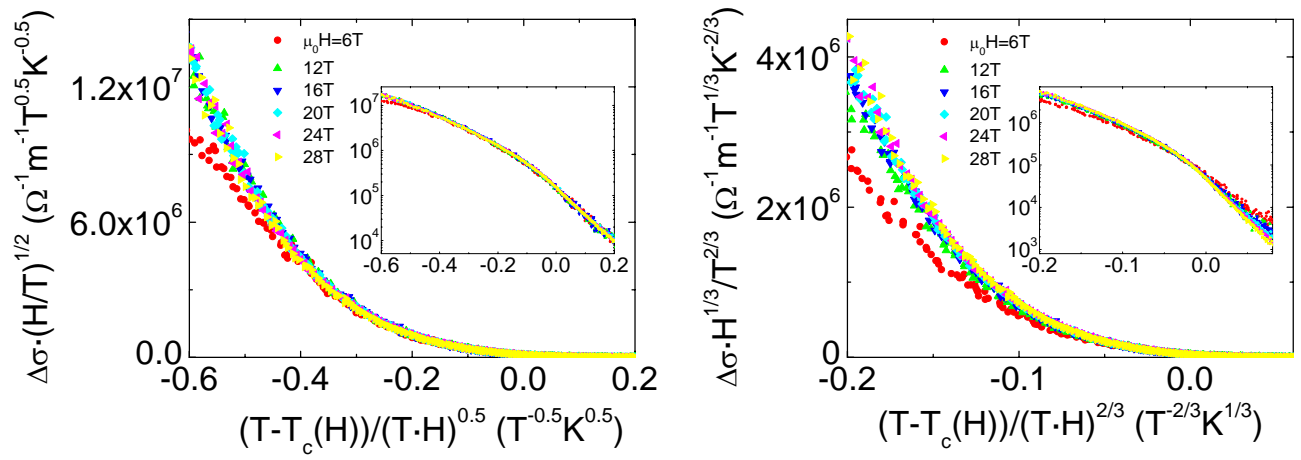


Figure 4

References

- ¹ Y.Kamihare, T.Watanabe, M.Hirano, H.Hosono, *J. Am. Chem. Soc.* 130, 3296 (2008)
- ² C.Wang, L.Li, S.Chi, Z.Zhu, Z.Ren, Y.Li, Y.Wang, X.Lin, Y.Luo, S.Jiang, X.Xu, G.Cao, Z.Xu, *Europhys. Lett.* 83, 67006 (2008)
- ³ J.Jaroszynski, S.C.Riggs, F.Hunte, A.Gurevich, D.C.Larbalestier, G.S.Boebinger, F.F.Balakirev, A.Migliori, Z.A.Ren, W.Lu, J.Yang, X.L.Shen, X.L.Dong, Z.X.Zhao, R.Jin, A.S.Sefat, M.A.McGuire, B.C.Sales, D.K.Christen, D.Mandrus, *Phys. Rev. B* 78, 064511 (2008)
- ⁴ Y.Jia, P.Cheng, L.Fang, H.Luo, H.Yang, C.Ren, L.Shan, C.Gu, H.H.Wen, *Appl. Phys. Lett.* 93, 032503 (2008)
- ⁵ U.Welp, R.Xie, A.E.Koshelev, W.K.Kwok, P.Cheng, L.Fang, H.H.Wen, *Phys. Rev. B* 78, 140510(R) (2008)
- ⁶ J.Jaroszynski, F.Hunte, L.Balicas, Y.J.Jo, I.Raicevic, A.Gurevich, D.C.Larbalestier, F.F.Balakirev, L.Fang, P.Cheng, Y.Jia, H.H.Wen, *Phys. Rev. B* 78, 174523 (2008)
- ⁷ R.H.Liu, G.Wu, T.Wu, D.F.Fang, H.Chen, S.Y.Li, K.Liu, Y.L.Xie, X.F.Wang, R.L.Yang, L.Ding, C.He, D.L.Feng, X.H.Chen, *Phys. Rev. Lett.* 101, 087001 (2008)
- ⁸ N.D.Zhigadlo, S.Katrych, Z.Bukowski, S.Weyeneth, R.Puzniak, J.karpinski, *J.Phys.:Condens. Matter* 20, 342202 (2008)
- ⁹ S.Weyeneth, U.Mosele, N.D.Zhigadlo, S.Katrych, Z.Bukowski, J.Karpinski, S.Kohout, J.Roos, H.Keller, in press on *J. Supercond. Nov. Magn.*
- ¹⁰ L.Balicas, A.Gurevich, Y.J.Jo, J.Jaroszynski, D.C.Larbalestier, R.H.Liu, H.Chen, X.H.Chen, N.D.Zhigadlo, S.Katrych, Z.Bukowski, J.Karpinski, arXiv:0809.4223
- ¹¹ A.Larkin, A.Varlamov, "Theory of Fluctuations in Superconductors", *The International Series of Monographs on Physics*, Clarendon Press, Oxford 2005, pages 31-35
- ¹² A.J.Drew, F.L.Pratt, T.Lancaster, S.J.Blundell, P.J.Baker, R.H.Liu, G.Wu, X.H.Chen, I.Watanabe, V.K.Malik, A.Dubroka, K.W.Kim, M.Rössle, C.Bernhard, *Phys. Rev. Lett.* 101, 097010 (2008)
- ¹³ R.Khasanov, H.Luetkens, A.Amato, H.H.Klauss, Z.A.Ren, J.Yang, W.Lu, Z.X.Zhao, *Phys. Rev. B* 78, 092506 (2008)
- ¹⁴ D.V.Livanov, A.A.Varlamov, M.Putti, M.R.Cimberle, C.Ferdeghini, *Eur. Phys. J. B* 18, 401 (2000)
- ¹⁵ L.G.Aslamazov, A.I.Larkin, *Phys. Lett.* 26A, 238 (1968)
- ¹⁶ W.J.Skocpol, M.Tinkham, *Rep. Prog. Phys.* 38, 1409 (1975)
- ¹⁷ W.E.Lawrence, S.Doniach, *Proceedings of the Twelfth International Conference on Low Temperature Physics*, Kyoto, 1970, edited by Eizo Kanda (Keigaku, Tokyo, 1971), p.361
- ¹⁸ M.B.Salamon, J.Shi, N.Overend, M.A.Howson, *Phys. Rev. B* 47, 5520 (1993)
- ¹⁹ P.A.Lee, S.R.Shenoy, *Phys. Rev. Lett.* 28, 1025 (1972)
- ²⁰ S.Ullah, A.T.Dorsey, *Phys. Rev. Lett.* 65, 2066 (1990)
- ²¹ S.Ullah, A.T.Dorsey, *Phys. Rev. B* 44, 262 (1991)
- ²² Z.Tešanovic, A.V.Andreev, *Phys. Rev. B* 49, 4064 (1994)
- ²³ Z.Tešanovic, L.Xing, L.Bulaevskii, Q.Li, M.Suenaga, *Phys. Rev. Lett.* 69, 3563 (1992)
- ²⁴ M.Roulin, A.Junod, E.Walker, *Physica C* 260, 257 (1996)
- ²⁵ U.Welp, S.Fleshler, W.K.Kwok, R.A.Klemm, V.M.Vinokur, J.Downey, B.Veal, G.W.Crabtree, *Phys. Rev. Lett.* 67, 3180 (1991)
- ²⁶ N.Overend, M.A.Howson, I.D.Lawrie, S.Abell, P.J.Hirst, C.Changkan, S.Chowdhury, J.W.Hodby, S.E.Inderhees, M.B.Salamon, *Phys. Rev. B* 54, 9499 (1996)
- ²⁷ D.H.Kim, K.E.Gray, M.D.Trochet, *Phys. Rev. B* 45, 10801 (1992)
- ²⁸ R.M.Costa, P.Pureur, L.Ghivelder, J.A.Campá, I.Rasines, *Phys. Rev. B* 56, 10836 (1997)
- ²⁹ S.W.Pierson, T.M.Katona, Z.Tešanovic, O.T.Valls, *Phys. Rev. B* 53, 8638 (1996)
- ³⁰ R.M.Costa, P.Pureur, M.Gusmão, S.Senoussi, K.Behnia, *Phys. Rev. B* 64, 214513 (2001)

-
- ³¹ A.Martinelli, M.Ferretti, P.Manfrinetti, A.Palenzona, M.Tropeano, M.R.Cimberle, C.Ferdeghini, R.Valle, M.Putti, A.S.Siri, *Supercond. Sci. Technol.* 21, 095017 (2008)
- ³² J.Jaroszynski, F.Hunte, L.Balicas, Y.J.Jo, I.Raicevic, A.Gurevich, D.C.Larbalestier, F.F.Balakirev, L.Fang, P.Cheng, Y.Jia, H.H.Wen, *Phys. Rev. B* 78, 174523 (2008)
- ³³ M.R.Cimberle, C.Ferdeghini, E.Giannini, D.Marré, M.Putti, A.S.Siri, F.Federici, A.Varlamov, *Phys. Rev. B* 55, R14745 (1997)
- ³⁴ S.W.Pierson, T.M.Katona, Z.Tešanovic, O.T.Valls, *Phys. Rev. B* 53, 8638 (1996)
- ³⁵ N.R.Werthamer, E.Helfand, P.C.Hohenberg, *Phys. Rev.* 147, 295 (1966)
- ³⁶ G.Fuchs, S.L.Drechsler, N.Kozlova, G.Behr, A.Köhler, J.Werner, K.Nenkov, C.Hess, R.Klingeler, J.E.Hamann-Borrero, A.Kondrat, M.Grobosch, A.Narduzzo, M.Knupfer, J.Freudenberger, B.Büchner, L.Schultz, *Phys. Rev. Lett.* 101, 237003 (2008)
- ³⁷ Y.Kohama, Y.Kamihara, S.A.Baily, L.Civale, S.C.Riggs, F.F.Balakirev, T.Atake, M.Jaime, M.Hirano, H.Hosono arXiv:0809.1133
- ³⁸ M.Putti, R.Vaglio, J.Rowell, *Supercond. Science and Tech.* 21, 043001 (2008)
- ³⁹ W.Bauhofer, W.Biberacher, B.Gegenheimer, W.Joss, R.K.Kremer, H.J.Mattausch, A.Muller, A.Simon, *Phys. Rev. Lett.* 63, 2520 (1989)
- ⁴⁰ M.Putti, M.R.Cimberle, C.Ferdeghini, G.Grassano, D.Marré, A.S.Siri, A.A.Varlamov, L.Correra, *Physica C* 314, 247 (1999)
- ⁴¹ M.Tropeano, C.Fanciulli, C.Ferdeghini, D.Marré, A.S.Siri, M.Putti, A.Martinelli, M.Ferretti, A.Palenzona, M.R.Cimberle, C.Mirri, S.Lupi, R.Sopracase, P.Calvani, A.Perucchi, *Supercond. Sci. Technol.* 22, 034004 (2009)